Digital Breast Tomosynthesis Reconstruction using Spatially Weighted Non-convex Regularization

Jiabei Zheng[*a,b], Jeffrey A. Fessler[a,b], Heang-Ping Chan[a]
[a]Department of Radiology, University of Michigan, Ann Arbor, MI 48109; [b] Department of Electrical Engineering and Computer Science, University of Michigan, Ann Arbor, MI 48109

ABSTRACT

Regularization is an effective strategy for reducing noise in tomographic reconstruction. This paper proposes a spatially weighted non-convex (SWNC) regularization method for digital breast tomosynthesis (DBT) image reconstruction. With a non-convex cost function, this method can suppress noise without blurring microcalcifications (MC) and spiculations of masses. To minimize the non-convex cost function, we apply a majorize-minimize separable quadratic surrogate algorithm (MM-SQS) that is further accelerated by ordered subsets (OS). We applied the new method to a heterogeneous breast phantom and to human subject DBT data, and observed improved image quality in both situations. A quantitative study also showed that the SWNC method can significantly enhance the contrast-to-noise ratio of MCs. By properly selecting its parameters, the SWNC regularizer can preserve the appearance of the mass margins and breast parenchyma.

Keywords: Digital Breast Tomosynthesis, Image Reconstruction, Non-Convex Regularization, Microcalcification Enhancement

1. INTRODUCTION

Digital breast tomosynthesis (DBT) has been developed to reduce the problem of overlapping tissue in conventional 2-D mammography. The total dose used in DBT is comparable to mammography; each projection is therefore low dose and relatively noisy. The noise can be amplified in the image reconstruction process, making it challenging to detect subtle microcalcification (MC) clusters and spiculated masses that are signs of early breast cancer. Regularization during reconstruction can control the noise, but it may also blur the MCs and the background tissue structures unless the regularization method is properly designed.

To improve the trade-off between spatial resolution and noise, we propose a new regularization method, referred to as the spatially weighted non-convex (SWNC) regularization method. The SWNC regularization method is inspired by the multi-scale bilateral filtering (MSBF) method that our group developed previously[1]. Both MSBF and SWNC consider the spatial and intensity differences between pixels within a small neighborhood centered at each pixel to estimate the presence of signal or noise. MSBF is a filtering method that one can use to post-process reconstructed images or one can apply it between each iteration of an iterative image reconstruction algorithm. Analyzing the resolution and noise properties of such inter-iteration filtering methods is challenging[2] particularly with nonlinear filtering methods. In contrast the SWNC regularizer is incorporated into the image reconstruction cost function in the problem formulation and then any suitable iterative algorithm can be applied to minimize that cost function. We focus on an MM-SQS algorithm with OS in this work.

In this paper, we first describe the mathematical form of the SWNC regularization. Then we propose a corresponding algorithm to reconstruct images by minimizing the non-convex cost function. Both phantom and human subject DBT were used to evaluate the effectiveness of the new method in enhancing MCs and preserving the quality of masses and tissue texture.

[*] Correspondence: jiabei@umich.edu

Medical Imaging 2016: Physics of Medical Imaging, edited by Despina Kontos, Thomas G. Flohr, Joseph Y. Luo,
Proc. of SPIE Vol. 9783, 978369 · © 2016 SPIE · CCC code: 1605-7422/16/$18 · doi: 10.1117/12.2216414

2. METHODS AND MATERIALS

2.1 Form of the Regularization

We pose DBT reconstruction as a regularized least-squares optimization problem:

$$\hat{\mathbf{f}} = \underset{\mathbf{f}}{\operatorname{argmin}} \frac{1}{2}\|\mathbf{y} - \mathbf{A}\mathbf{f}\|_2^2 + \beta R_{\mathrm{b}}(\mathbf{f})$$

where **f** is the image to be reconstructed, **y** is the measured projection views (PV), **A** is the system matrix and β is the regularization parameter that influences the resolution-noise trade-off. Note that both **y** and **A** contain all projection angles, namely if there are *N* projection angles, we have the following expression:

$$\mathbf{A} = \begin{pmatrix} \mathbf{A}_1 \\ \cdots \\ \mathbf{A}_N \end{pmatrix}, \quad \mathbf{y} = \begin{pmatrix} \mathbf{y}_1 \\ \cdots \\ \mathbf{y}_N \end{pmatrix}$$

where $\mathbf{A}_{\mathrm{i}}$ denotes the system matrix for the *i*th projection view and $\mathbf{y}_{\mathrm{i}}$ denotes the *i*th measured projection view.

Inspired by our previous method of using MSBF[1] between iterations to regularize the noise, we design the regularizer to be the sum of the product of two terms, one depends on the spatial distance between the pixel of interest and the pixels in a neighborhood $N_{\vec{n}}$, and the other depends on the intensity difference between the same pixels. Specifically, the SWNC regularizer has the following form:

$$R_{\mathrm{b}}(\mathbf{f}) = \sigma_r^2 \sum_{\vec{n}} \sum_{\vec{n}' \in \mathcal{N}_{\vec{n}}} \exp\left(-\frac{\|\vec{r}[\vec{n}] - \vec{r}[\vec{n}']\|_2^2}{2\sigma_d^2}\right)\left(1 - \frac{1}{1 + (\mathbf{f}[\vec{n}] - \mathbf{f}[\vec{n}'])^2/2\sigma_r^2}\right)$$

The regularizer has two parameters σ_d and σ_r. Essentially, σ_d controls the feature size to be smoothed, and σ_r is a soft threshold that controls whether a fluctuation in intensity is treated as noise or signal. The intensity part uses the Geman-McClure function[3] $\left(1 - \frac{1}{1+t^2}\right)$ as shown in Figure 1. This non-convex function increases slowly when *t* is beyond a threshold and is upper bounded by 1. Thus $R_{\mathrm{b}}(\mathbf{f})$ no longer increases as the intensity difference between the neighboring pixels is large enough. The data-fitting term $\|\mathbf{y} - \mathbf{A}\mathbf{f}\|_2^2$ in the cost function is therefore able to enhance the strength of a signal without being constrained by $R_{\mathrm{b}}(\mathbf{f})$ as long as the signal is strong enough. Thus the SWNC regularization can suppress noise without degrading the strength of MCs and mass margins and spiculations.

In DBT reconstruction, the slice thickness is much larger than the in-plane pixel size. Correlation between neighboring slices is relatively weak. Thus, we apply the regularization to each slice separately. In our DBT application, we used a 9×9 pixel neighborhood $N_{\vec{n}}$, based on consideration of feature sizes in DBT and the computational cost.

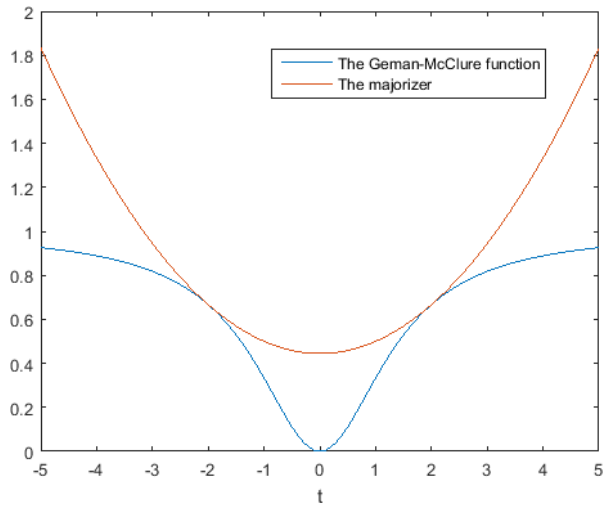

Figure 1. The Geman-McClure function and its corresponding majorizer at $t_0 = 2$.

2.2 Algorithm for Minimizing the Non-Convex Cost Function

In principle, the SWNC regularization is related to non-local means (NLM) regularization. Unlike some existing NLM regularization methods[4, 5], the SWNC method does not rely on a pre-calculated weight map. Inspired by the framework for non-local regularization[6], we use the majorize-minimize algorithm (MM algorithm)[7] for minimizing this non-convex cost function. A quadratic majorizer (as shown in Figure 1) of $\left(1-\frac{1}{1+t^2}\right)$ about a point t_0 is:

$$1-\frac{1}{1+t^2}<\frac{1}{2}\left(\frac{1}{1+t_0^2}\right)^2(t^2-t_0^2)+\text{const}(t_0)$$

As a result, denoting the current estimate of the image to be $\mathbf{f}^{(k)}$, we majorize $R_{\text{b}}(\mathbf{f})$ by the following function:

$$\Phi_{\text{b}}(\mathbf{f},\mathbf{f}^{(k)})=\frac{1}{2}\sum_{\vec{n}}\sum_{\vec{n}'\in\mathcal{N}_{\vec{n}}}\exp\left(-\frac{\|\vec{r}[\vec{n}]-\vec{r}[\vec{n}']\|_2^2}{2\sigma_d^2}\right)\left(\frac{1}{1+(\mathbf{f}^{(k)}[\vec{n}]-\mathbf{f}^{(k)}[\vec{n}'])^2/2\sigma_r^2}\right)^2(\mathbf{f}[\vec{n}]-\mathbf{f}[\vec{n}'])^2+\text{const}(\mathbf{f}^{(k)})=\frac{1}{2}\|\mathbf{Cf}\|_{\mathbf{W}^{(k)}}^2+\text{const}(\mathbf{f}^{(k)})$$

where k denote the MM iteration and $\mathbf{C}$ represents all finite difference operations within the neighborhood $N_{\vec{n}}$ (written in a column). To minimize $\Phi_{\text{b}}(\mathbf{f},\mathbf{f}^{(k)})$ in the following quadratic optimization problem:

$$\mathbf{f}^{(k+1)}=\underset{\mathbf{f}}{\text{argmin}}\,\Phi_b(\mathbf{f},\mathbf{f}^{(k)})$$

we used the separable quadratic surrogate algorithm (SQS)[8]. Each SQS iteration is accelerated with ordered-subset (OS)[9] where only one PV is used in each update. Let l denote the SQS index and i denote the PV index, we implemented the MM-OS-SQS algorithm as the following triple loop:

$$\mathbf{f}^{(k+1,l,i+1)}=\mathbf{f}^{(k+1,l,i)}-(N\mathbf{A}_i^{\text{T}}(\mathbf{A}_i\mathbf{f}^{(k+1,l,i)}-\mathbf{y}_i)+\beta\mathbf{C}^{\text{T}}\mathbf{W}^{(k)}\mathbf{C}\mathbf{f}^{(k+1,l,i)})\oslash\mathbf{D}^{(k)}$$

where N denotes the number of PVs and the step size is controlled by:

$$\mathbf{D}^{(k)}=\mathbf{A}^{\text{T}}\mathbf{A}\mathbf{1}+\left|\mathbf{C}^{\text{T}}\right|\mathbf{W}^{(k)}|\mathbf{C}|\,\mathbf{1}$$

where $\mathbf{1}$ is a vector with all unity components. The SQS index l is increased by 1 after all projections have been used once. $\mathbf{D}^{(k)}$ is only updated after the majorizing function $\Phi_{\text{b}}(\mathbf{f},\mathbf{f}^{(k)})$ converges. Then the next MM iteration starts and the index k is increased by 1.

We initialize the image $\mathbf{f}$ with the reconstructed image resulting from one iteration of the simultaneous algebraic reconstruction technique (SART)[10, 11]. We select σ_r based on the standard deviation of a noise patch after one SART iteration: $\sigma_r=\kappa_r\sigma_{\text{noise patch}}$, where κ_r is a proportionality constant that controls the estimation of whether the intensity change at a pixel is noise or signal. We will mainly use κ_r in the following discussion.

2.3 Figures of Merit

We applied the SWNC regularization method using MM-OS-SQS to DBTs of both breast phantom and human subjects. The phantom consisted of a stack of five 1-cm-thick 50% adipose/50% glandular heterogeneous slabs that simulated the composition and parenchymal pattern of the breast[12]. Clusters of calcium carbonate specks of three nominal size ranges (0.25-0.30 mm, 0.18-0.25 mm, and 0.15-0.18 mm) simulated MCs of different conspicuity levels. Several clusters of each contrast group were sandwiched at random locations between the slabs. The DBT system acquired 21 projections in 3^{o} increments over a 60^{o} arc using a flat panel CsI/a:Si detector with a pixel pitch of $0.1\text{mm}\times 0.1\text{mm}$. All DBTs were reconstructed at $0.1\text{mm}\times 0.1\text{mm}$ pixel size and 1 mm slice spacing.

Two figures of merits were used for quantitative comparison of reconstruction quality: contrast-to-noise ratio (CNR) and full-width at half maximum (FWHM). Computations of CNR and FWHM were based on least-squares fitting of a 2-D isotropic Gaussian function to each individual MC. With the fitted standard deviation σ_{MC}, the FWHM is given by $2.355\sigma_{\text{MC}}$. The noise level σ_{NP} is estimated from a noise patch near each cluster. The CNR is given as: $\text{CNR}=A_{\text{MC}}/\sigma_{\text{NP}}$, where A_{MC} is the fitted amplitude of the MC. The mean and standard deviation of each measurement were estimated from over 18 MCs for each size range.

We compared three different reconstruction methods: (1) non-regularized SART, (2) SART with MSBF[1], and (3) the new SWNC regularization method using MM-OS-SQS. Based on the previous studies, 2 iterations are chosen for both the non-regularized SART and SART-MSBF methods. For the SWNC method with MM-OS-SQS, 2 MM iterations, each including 4 SQS iterations, were chosen for comparison.

3. RESULTS

Figure 2 shows the reconstructed MC clusters. SWNC enhanced the visibility of the MCs more strongly than the other two methods. Quantitatively, the CNR of the subtlest MCs (0.15-0.18 mm) has increased by 92.5% compared with SART-MSBF (Figure 3), and by 121.8% compared with non-regularized SART. With SWNC, the FWHMs of the MCs decreased, indicating better MC sharpness. However, the variations of the CNR after SWNC enhancement are greater than those of the other methods as indicated by the larger error bars (±1 standard deviation) of CNR with SWNC. We are investigating better design of the regularization method to achieve more uniform enhancement for subtle MCs.

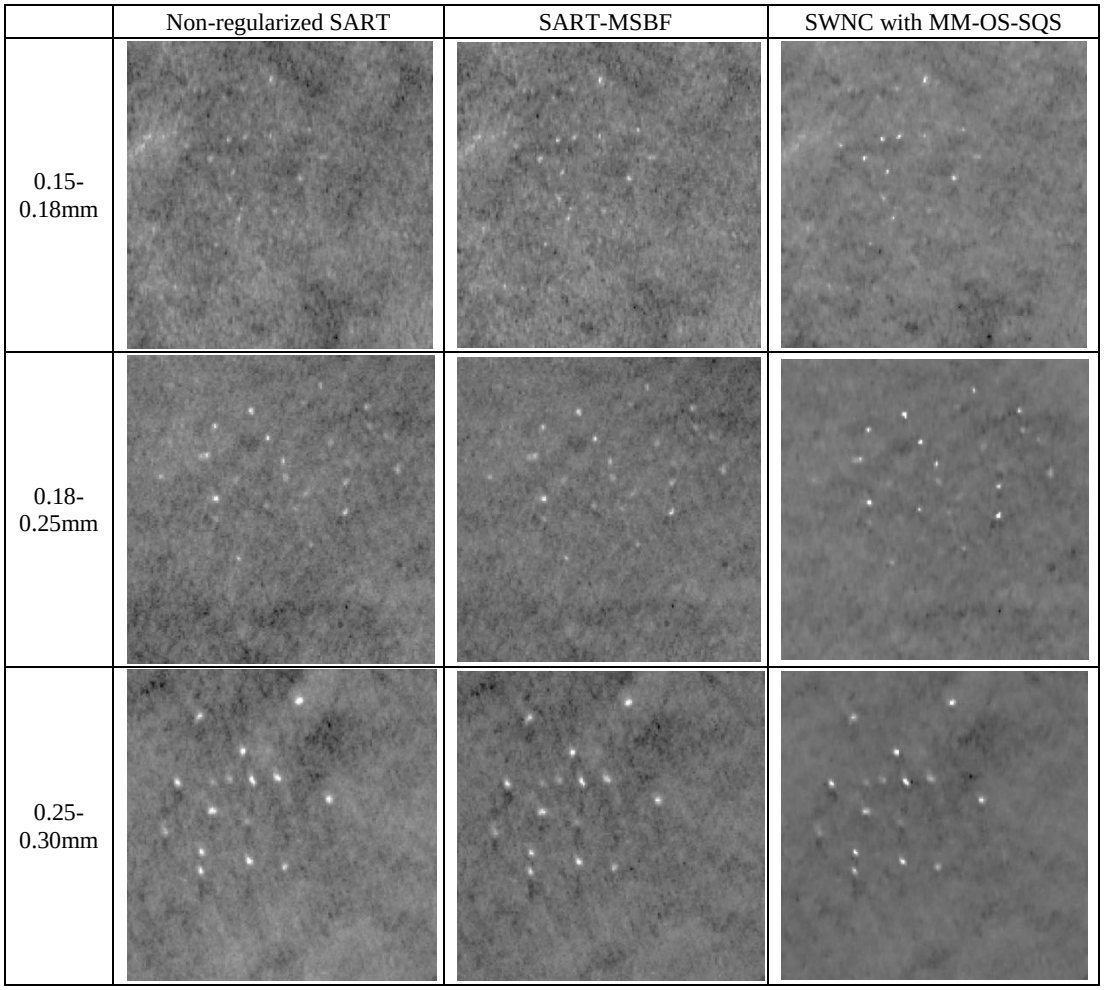

Figure 2. Simulated MC clusters of different sizes in breast phantom DBT reconstructed with three different methods. All ROIs are 160 x 160 pixels in size (1 pixel = 0.1 mm). The SWNC parameters were chosen as: $\sigma_d = 0.16\ mm$, $\kappa_r = 2.6$ and $\beta = 3\ mm^2$.

Parameter selection is important for good performance of the SWNC regularization. Figure 4 shows plots of CNR and FWHM as one of the three parameters (κ_r, σ_d and β) was varied. Different sized MCs require different κ_r, σ_d and β to achieve maximum CNR. The horizontal lines marked with 'SART-MSBF' represent the values achieved with the SART-MSBF method. The SWNC method outperforms the SART-MSBF method under most conditions in the sense of enhancing CNR. However, as κ_r, σ_d or β increased, the FWHMs of the small MCs increased, approaching those of the larger MCs, indicating the small MCs were blurred.

CNR only estimates the intensity of MCs relative to noise. Parameters that maximize CNR actually can generate artifacts such as salt-and-pepper noise in the image and patchy appearances of the breast parenchyma and along the spiculations. We visually inspected the images reconstructed with different parameters to look for parameters that enhance MCs while preserving background structures. Empirically, we decided that the combination of parameters $\sigma_d = 0.16\ mm$, $\kappa_r = 2.6$ and $\beta = 3\ mm^2$ is a good choice that generated good-quality images with obvious enhancement of MCs, as demonstrated by the images in Figure 2.

We also applied the SWNC by the MM-OS-SQS method with the same set of parameters to human subject DBT (Figure 5). The SWNC method suppressed noise, enhanced MCs and preserved the appearance of the spiculations and the breast parenchyma. The human subject DBT result shows the potential of the SWNC method in improving the detectability of MC clusters by either radiologists or computer aided diagonis (CAD) systems[13-15].

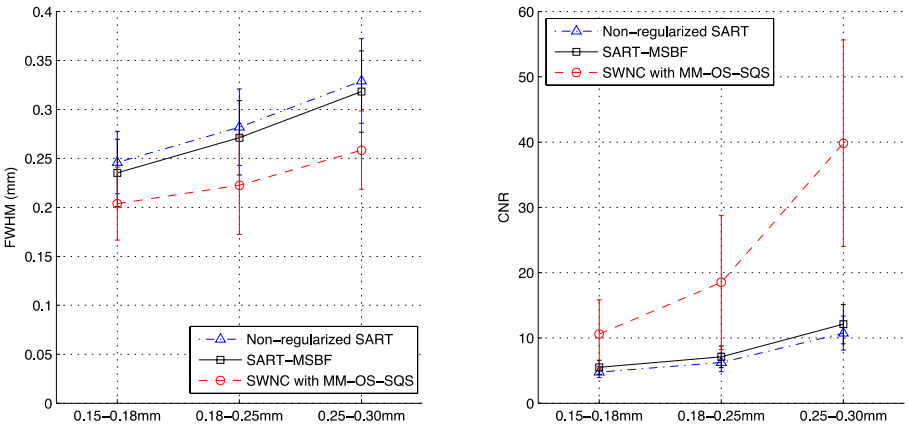

Figure 3. FWHM and CNR of MCs with different reconstruction methods. Compared with SART and SART-MSBF, the SWNC method increases mean CNR and decreases mean FWHM. The SWNC parameters were chosen as: $\sigma_d = 0.16\ mm$, $\kappa_r = 2.6$ and $\beta = 3\ mm^2$. With SWNC, the degree of enhancement in CNR for MCs varies over a wide range as indicated by the error bars (±1 standard deviation), which can also be seen in the image examples in Fig. 2.

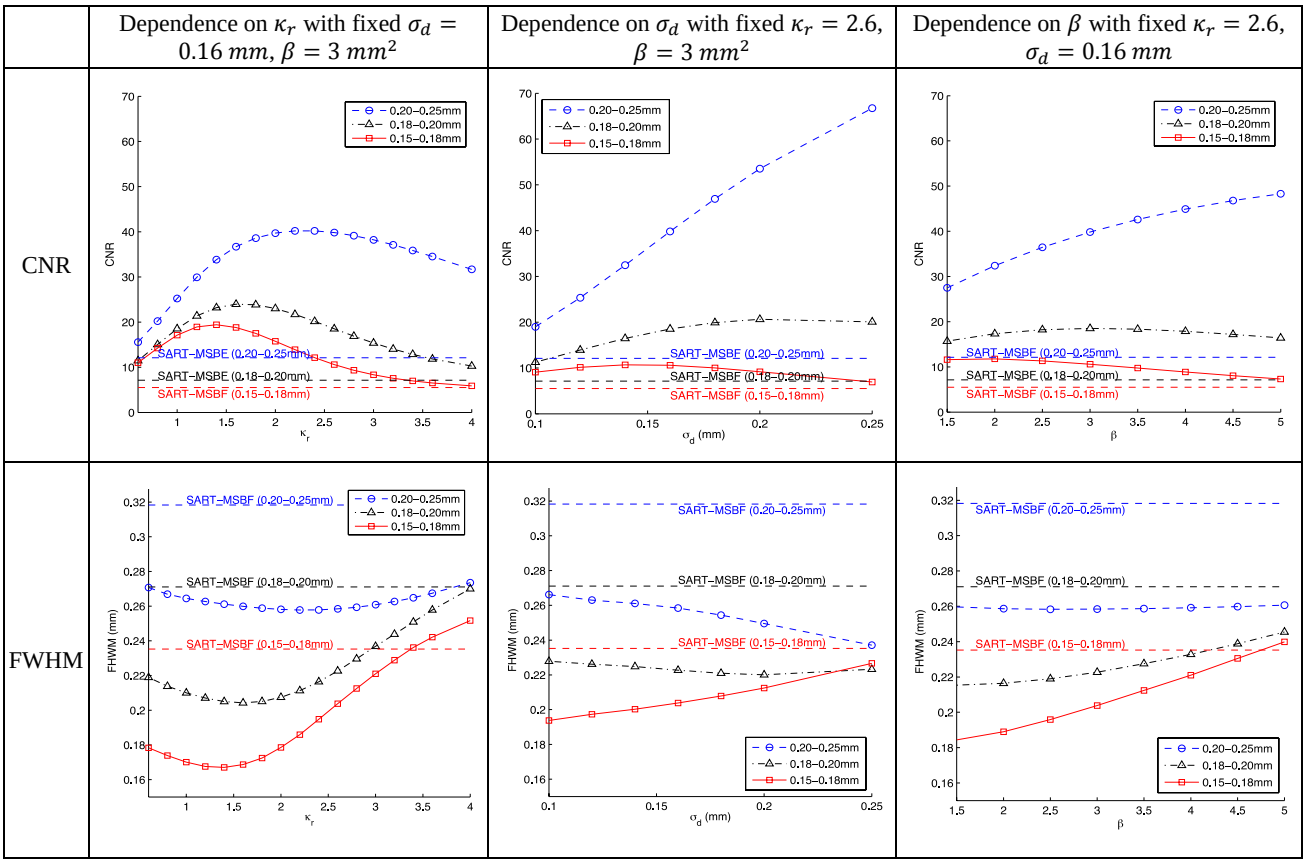

Figure 4. Parameter optimization: dependence of mean CNR and mean FWHM on κ_r, σ_d or β. For clarity, the error bars were not plotted.

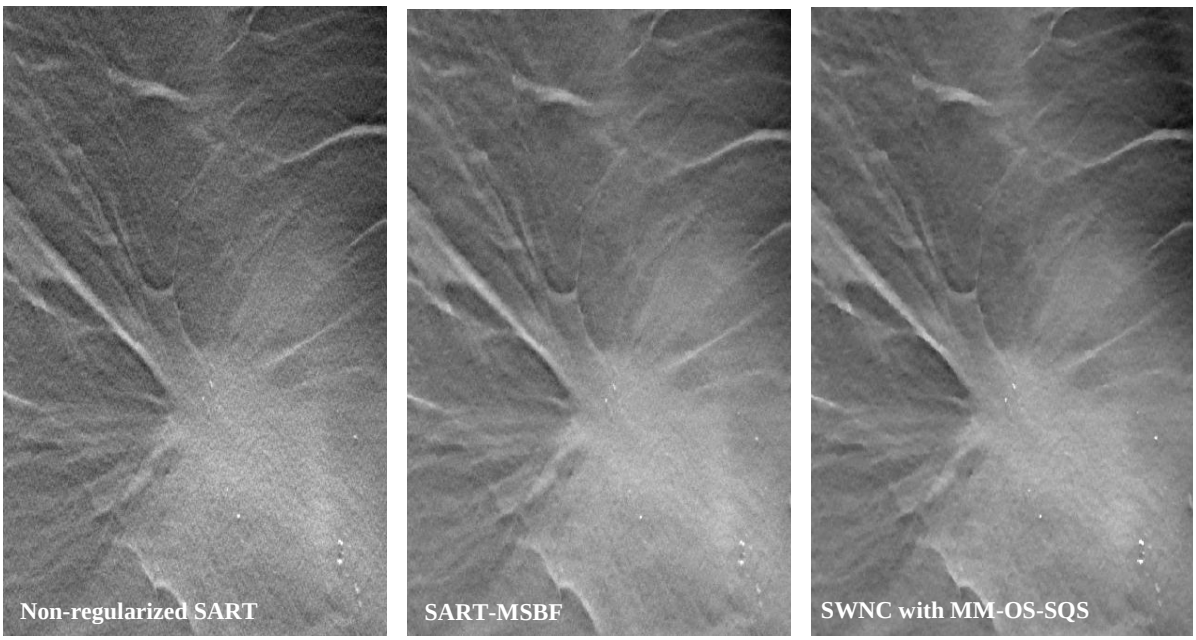

Figure 5. Comparison of the three methods for the DBT of a human subject with a spiculated mass and MCs. The SWNC parameters were chosen as: $\sigma_d = 0.16\ mm$, $\kappa_r = 2.6$ and $\beta = 3\ mm^2$. The breast parenchyma is very noisy in the non-regularized SART image. The noise is reduced by SART-MSBF and further by our new SWNC method.

4. CONCLUSIONS

In this paper, we proposed an SWNC regularization method for DBT and implemented an MM-OS-SQS algorithm to reconstruct DBT images. The new method is able to achieve strong enhancement of MCs relative to noise while preserving the appearance of the spiculations and the breast parenchyma for both breast phantom and patient DBTs. A major limitation is the large variations in the CNR of different MCs in the DBTs reconstructed with the SWNC method. Parameter selection is also important for obtaining good results. Study is underway to further improve the SWNC regularized reconstruction of DBT.

ACKNOWLEDGEMENTS

This work is supported by National Institutes of Health grant number R01 CA151443.

REFERENCES

[1] Y. Lu, H.-P. Chan, J. Wei *et al.*, "Multiscale Bilateral Filtering for Improving Image Quality in Digital Breast Tomosynthesis," Medical Physics, 42(1), 182-195 (2015).
[2] S. Mustafovic, and K. Thielemans, "Object dependency of resolution in reconstruction algorithms with interiteration filtering applied to PET data," Ieee Transactions on Medical Imaging, 23(4), 433-446 (2004).
[3] S. Geman, and D. McClure, "Bayesian image analysis: An application to single photon emission tomography," Proceedings of the American Statistical Association Statistical Computing Section, 12-18 (1985).
[4] G. Peyre, S. Bougleux, and L. Cohen, "Non-local Regularization of Inverse Problems," Proceedings of the European Conference on Computer Vision (ECCV 2008), 57-68 (2008).
[5] G. B. Wang, and J. Y. Qi, "Patch-Based Regularization for Iterative PET Image Reconstruction," 2011 8th IEEE International Symposium on Biomedical Imaging: From Nano to Macro, 1508-1511 (2011).
[6] Z. L. Yang, and M. Jacob, "Nonlocal Regularization of Inverse Problems: A Unified Variational Framework," IEEE Transactions on Image Processing, 22(8), 3192-3203 (2013).
[7] D. R. Hunter, and K. Lange, "Quantile regression via an MM algorithm," Journal of Computational and Graphical Statistics, 9(1), 60-77 (2000).
[8] D. Kim, D. Pal, J. B. Thibault *et al.*, "Accelerating ordered subsets image reconstruction for X-ray CT using spatially nonuniform optimization transfer," IEEE Trans Med Imaging, 32(11), 1965-78 (2013).
[9] H. Erdogan, and J. A. Fessler, "Ordered subsets algorithms for transmission tomography," Physics in Medicine and Biology, 44, 2835-2851 (1999).
[10] A. H. Andersen, and A. C. Kak, "Simultaneous algebraic reconstruction technique (SART): a new implementation of the ART algorithm," Ultrason. Imaging, 6, 81-94 (1984).
[11] Y. Zhang, H.-P. Chan, B. Sahiner *et al.*, "A comparative study of limited-angle cone-beam reconstruction methods for breast tomosynthesis," Medical Physics, 33(10), 3781-3795 (2006).
[12] H. P. Chan, M. M. Goodsitt, M. A. Helvie *et al.*, "Digital Breast Tomosynthesis: Observer Performance of Clustered Microcalcification Detection on Breast Phantom Images Acquired with an Experimental System Using Variable Scan Angles, Angular Increments, and Number of Projection Views," Radiology, 273(3), 675-685 (2014).
[13] R. K. Samala, H. P. Chan, Y. Lu *et al.*, "Computer-aided detection of clustered microcalcifications in multiscale bilateral filtering regularized reconstructed digital breast tomosynthesis volume," Medical Physics, 41(2), 021901 (2014).
[14] R. K. Samala, H.-P. Chan, Y. Lu *et al.*, "Computer-aided Detection System for Clustered Microcalcifications in Digital Breast Tomosynthesis using Joint Information from Volumetric and Planar Projection Images," Physics in Medicine and Biology, 60(21), 8457-8479 (2015).
[15] R. K. Samala, H. P. Chan, Y. Lu *et al.*, "Digital breast tomosynthesis: computer-aided detection of clustered microcalcifications on planar projection images," Physics in Medicine and Biology, 59(23), 7457-7477 (2014).